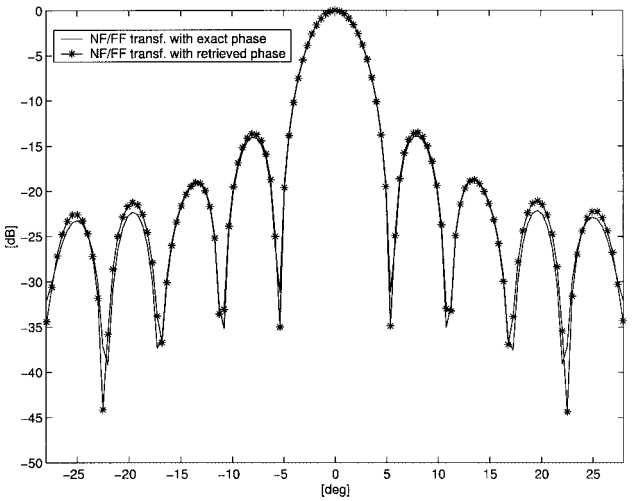

Figure 5 Far-field amplitude (θ component in the y–z plane)

REFERENCES

1. T. Isernia, G. Leone, and R. Pierri, Radiation pattern evaluation from near-field intensities on planes, IEEE Trans Antennas Propagat 44 (1996), 701–710.
2. R. Pierri, G. D'Elia, and F. Soldovieri, A two probes scanning phaseless near-field far-field transformation technique, IEEE Trans Antennas Propagat 47 (1999), 792–802.
3. S. Costanzo and G. Di Massa, An integrated probe for phaseless near-field measurements, submitted.
4. Y. Rahmat-Samii, V. Galindo-Israel, and R. Mittra, A plane-polar approach for far-field construction from near-field measurements, IEEE Trans Antennas Propagat AP-28 (1980), 216–230.
5. O.M. Bucci, C. Gennarelli, and C. Savarese, Fast and accurate near-field far-field transformation by sampling interpolation of plane-polar measurements, IEEE Trans Antennas Propagat 39 (1991), 48–55.
6. M.S. Gatti and Y. Rahmat-Samii, FFT applications to plane-polar near-field antenna measurements, IEEE Trans Antennas Propagat 36 (1988), 781–791.

BROADSIDE COUPLINGS FOR HIGH-SELECTIVITY MICROSTRIP FILTERS

Alejandro Alvarez Melcón,[1] Juan R. Mosig,[1] and Marco Guglielmi[2]

[1]Laboratoire d'Electromagnetisme et d'Acoustique
Ecole Polytechnique Fédérale de Lausanne
Lausanne CH-1015, Switzerland
[2]European Space Research and Technology Center (ESTEC)
2200AG Noordwijk, The Netherlands

Received 21 March 2001

ABSTRACT: *This paper describes a number of broadside-coupled microstrip structures and their use for the implementation of high-selectivity multilayered filters. The broadside configuration allows for the introduction of cross couplings between nonadjacent resonators. The cross couplings can then be used to implement transmission zeros that can significantly increase the selectivity of the filters. Furthermore, the investigation shows that the amount of coupling can be considerably increased if the resonators are broadside coupled, thus easily allowing the implementation of broadband filters. Measured results are shown to agree with predictions, thereby fully validating the new structures described.* © 2001 John Wiley & Sons, Inc. Microwave Opt Technol Lett 30: 295–302, 2001.

Key words: *microwave filters; integral equation; transmission zeros; multilayered circuits; broadside couplings*

1. INTRODUCTION

The development of microstrip filters remains a very important activity in many communication applications [1–3]. Great effort is being directed toward the investigation of new filter configurations exhibiting better electrical performances [4, 5], including the use of high-temperature superconductors [6–8]. In this context, the filter selectivity is a key parameter that must always be increased in order to better use the available spectrum, and to provide protection from unwanted signals.

A well-established technique for increasing the selectivity of microwave filters is the implementation of transmission zeros in the insertion loss response. In the case of waveguide filters, many implementations have been successfully developed in the past [9–14]. In the case of microstrip filters, several works can also be found in the technical literature describing techniques to increase the filter selectivity. Recently, a work has been published on this subject, which presents a printed structure with a single pair of transmission zeros at finite frequencies [15]. The presented structure is composed of square open-loop resonators which are side coupled, and the desired transmission zeros are obtained by classical cross-coupling interactions between nonadjacent resonators. Although the proposed approach is indeed valid, the total surface occupied by the circuit rapidly increases since the square resonators are placed following a meander line in order to allow for the introduction of the side cross-coupling effects. The work proposed in [15] is based on previous works by Hong and Lancaster [16] and Yu and Chang [17], in which elliptic transfer functions are also implemented by using the same square open-loop resonators combined with cross couplings between nonadjacent resonators, but they are always side coupled. Another example of a printed filter which uses side cross-coupling interactions can be found in [18], where hairpin resonators are placed in a square matrix to achieve an elliptic transfer function for a second-order filter.

As regards broadside-coupled printed structures, a few recent examples can be found in the technical literature, showing the increasing interest in these configurations. For instance, [19] describes a printed structure in which two line resonators are broadside coupled to two slot resonators in order to implement wide-frequency spurious-free response characteristics. Also, in [20], a broadside coupler is designed and successfully tested using integrated MMIC multilayer technology. Another useful example can be found in [21], where an elliptic transfer function is synthesized for a second-order filter by broadside coupling two resonators through a slot open on the common ground plane. This idea of introducing coupling through a slot open on the common ground plane is also used in [22], in conjunction with the already mentioned square open-loop resonators, to implement elliptic transfer functions with a more compact configuration than the original one proposed in [16]. Other works utilizing aperture couplings on the common ground between layers can be found in [23] or [24], for instance.

In this contribution we will further investigate broadside-coupled structures for high-performance microwave filters. In the paper, we first describe a fast and accurate software tool for the analysis of multilayer planar circuits [25], and then investigate several broadside-coupled microstrip filter configurations to explore novel possibilities of implementing transmission zeros. It is demonstrated that transmission zeros

can be generated not only by introducing classical cross-coupling effects between nonadjacent resonators, but also by using the interactions between the different modes excited. Using these interactions, the position of the transmission zeros can be controlled by acting on the dispersion properties of the relevant modes. Furthermore, the use of broadside configurations results in a considerably increased coupling between resonators, thus allowing for the implementation of broadband filters, as already pointed out in [22]. In addition to simulations, several comparisons between measured and predicted results are also presented. The good agreement between theoretical predictions and measurements shows that the structures proposed are indeed feasible, and that transmission zeros can be efficiently implemented and controlled.

2. THEORY

For the structures investigated in the present paper, a software tool based on a spatial integral equation formulation, as developed in [25], has been used. Full details of the formulation can be found in [25], so they will not be repeated here. For the sake of completeness, however, the most relevant features on which the software tool is based will now be briefly presented.

The basic structure under investigation is composed of an arbitrary number of metallic lines printed on an arbitrary number of dielectric layers as shown in Figure 1. The whole structure is shielded by a metallic enclosure, and the analysis is restricted, as mentioned in [25], to unconnected rectangular metallic areas.

The integral equation formulation starts with the imposition of the boundary conditions for the electromagnetic fields in the structure. After imposition of a vanishing tangent electric field in all of the n-metallic areas, a coupled system of integral equations is obtained [25]. The kernel of this integral equation is formed with the spatial-domain boxed Green's functions of the multilayered medium. In [25], these Green's functions are formulated using an infinite series of waveguide modes, with the coefficients of the expansion given by the voltages in equivalent transverse transmission-line networks.

The numerical solution of the system of integral equations is obtained using a Galerkin implementation of the method of moments (MoM).

The resulting software can perform the analysis of the structures involved in a few seconds per frequency point (depending on the actual complexity of the geometry), and is rigorous, so that all of the coupling phenomena taking place in the structure can be accurately modeled.

3. APPLICATIONS

The implementation of microstrip filters using sections of side-coupled lines has been known for some time, and the associated design techniques are now very well mastered [26, 27]. An alternative configuration to side-coupled filters is the broadside-coupled structure.

Following this concept, each resonator of the filter is printed on a different substrate, and it is coupled broadside to the other resonators, as shown in Figure 2. An important advantage of this configuration with respect to the side-coupled structure is that the lateral dimensions of the filter are greatly reduced. Another advantage is that the amount of coupling between the resonators is naturally increased in the broadside configuration. As a consequence, the very narrow gaps usually required to couple the resonators in broadband side-coupled filters [28] are avoided.

In many applications, low weight and size are important requirements to be respected. The size of the previous filter can be further reduced if the resonators of the structure are connected to the walls of the box. In this way, the walls act as electrical mirrors for the resonators, and their physical sizes are thus reduced in half. This is shown in the filter structure of Figure 3, where we show a microwave filter exhibiting essentially the same electrical response as before, but with

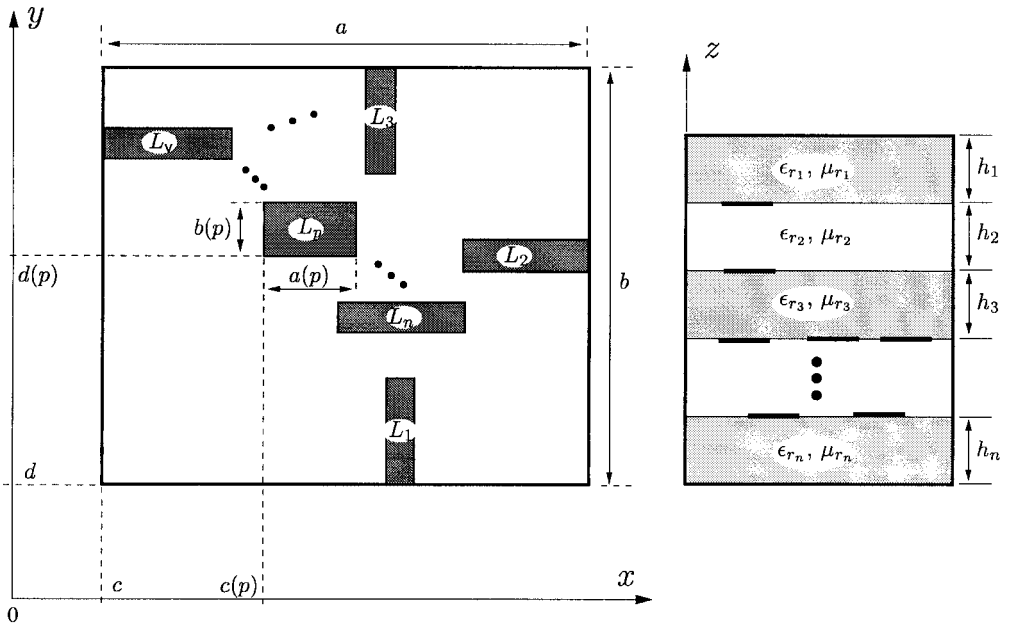

Figure 1 General boxed multilayered microwave printed circuit composed of an arbitrary number of metallic lines, analyzed in this paper

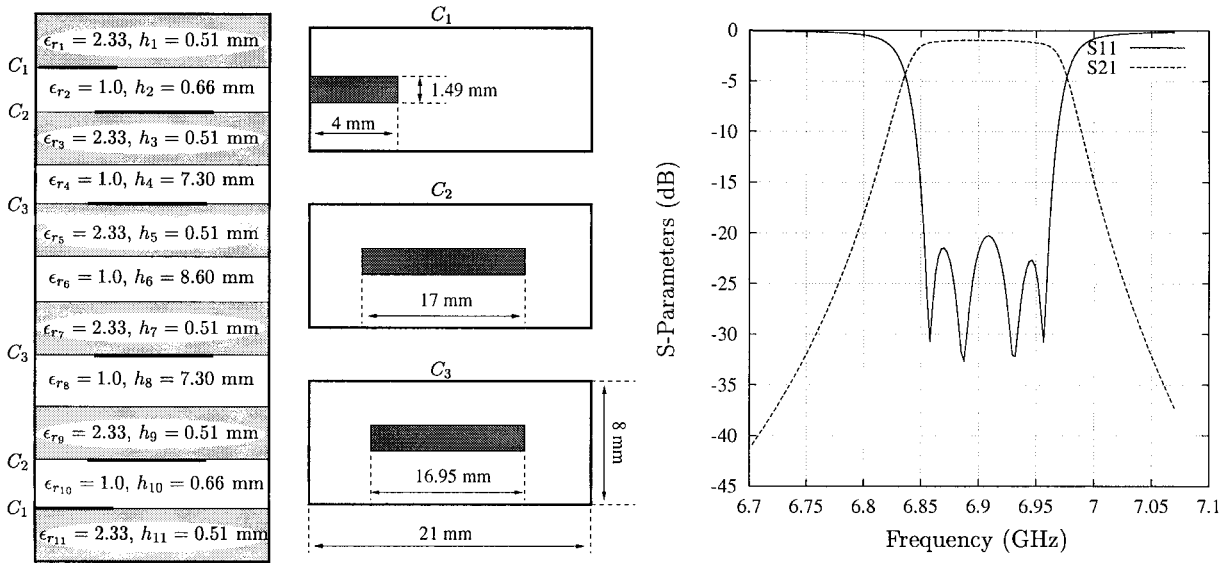

(a) Geometry of the filter. **(b)** Electrical response.

Figure 2 Response of the broadside-coupled filter after optimization

the size of the structure reduced by half. This configuration is essentially the microstrip equivalent of a comb-line filter in a metallic waveguide [29–31].

A similar idea of connecting the resonators to the walls of the cavity can also be used for the implementation of very compact interdigital filters. In this case, the resonators are connected to opposite walls alternatively, as shown in Figure 4. In addition, a broadband operation is achieved by implementing the input and output couplings of the filter using the broadside concept (see Fig. 4). To show the feasibility of this structure, the filter was manufactured and tested, and Figure 4(b) presents the measured versus simulated results, showing good agreement. For the practical realization of the filter, small wires were connected to the walls of the cavity in order to assure good contact for the implementation of the short-circuited resonators.

The broadside coupling concept previously described can also be used to introduce cross couplings between nonadjacent resonators, thus resulting in the implementation of transmission zeros [21].

It is well known that a single transmission zero can be implemented by introducing a cross coupling between the first and third resonators in a third-order filter [32]. Moreover, the position of the transmission zero with respect to the passband depends on the sign of the cross-coupling introduced. Figure 5 shows a multilayered filter with a transmis-

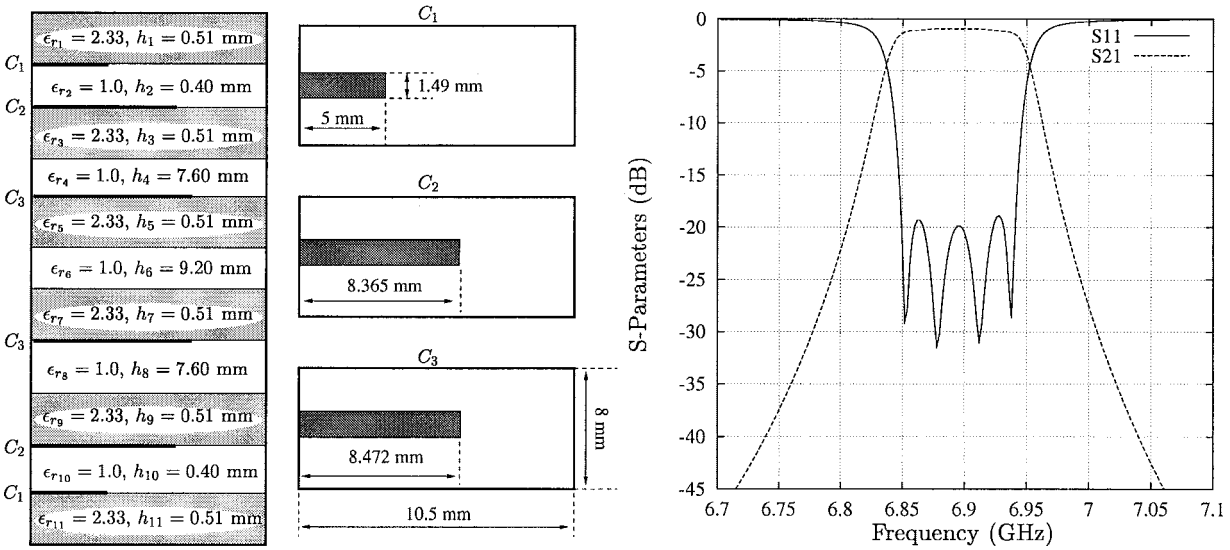

(a) Geometry of the filter. **(b)** Electrical response.

Figure 3 Response of the broadside-coupled filter with resonators connected to a wall

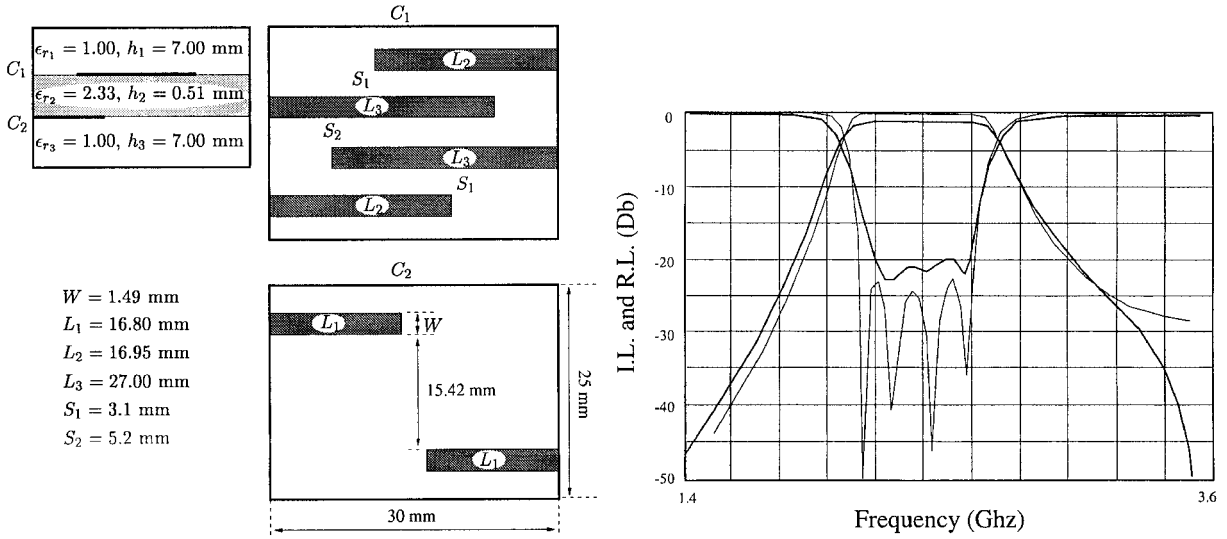

(a) Geometry of the filter.

(b) Measured versus simulated results.

Figure 4 Interdigital filter with broadside input coupling. Thin lines are simulations, while thick lines are measurements

sion zero above the passband using the 1–3 cross-coupling concept. As shown in Figure 5, the second resonator is printed on a different substrate, and it is coupled broadside to allow the introduction of a cross coupling between the first and third resonators (see Fig. 5). In order to easily realize this structure, the two dielectrics used to print the resonators are separated by a foam material of dielectric constant close to unity ($\epsilon_r = 1.07$). Figure 5(b) presents the measured versus simulated results, showing that the measured transmission zero is indeed close to the expected location predicted by the simulation tool.

It is interesting to notice that, in this structure, the box has a general shielding effect on the circuit, but it does not play an important role in the generation of the transmission zero, which is only produced by the cross coupling introduced between the first and third resonators. To demonstrate this fact, a similar filter structure has been designed and manufactured, but considering substrates with infinite lateral transverse dimensions (no lateral walls). Figure 6 presents the structure together with measured versus simulated results, again showing good agreement. In particular, the transmission zero is positioned again at the desired frequency, close to the expected location. Only the measured out-of-band response of the filter contains a spurious behavior, probably due to the finite dimensions of the dielectric in the real manufactured prototype.

The main problem of the structure just presented is the difficulty in placing a transmission zero below the passband

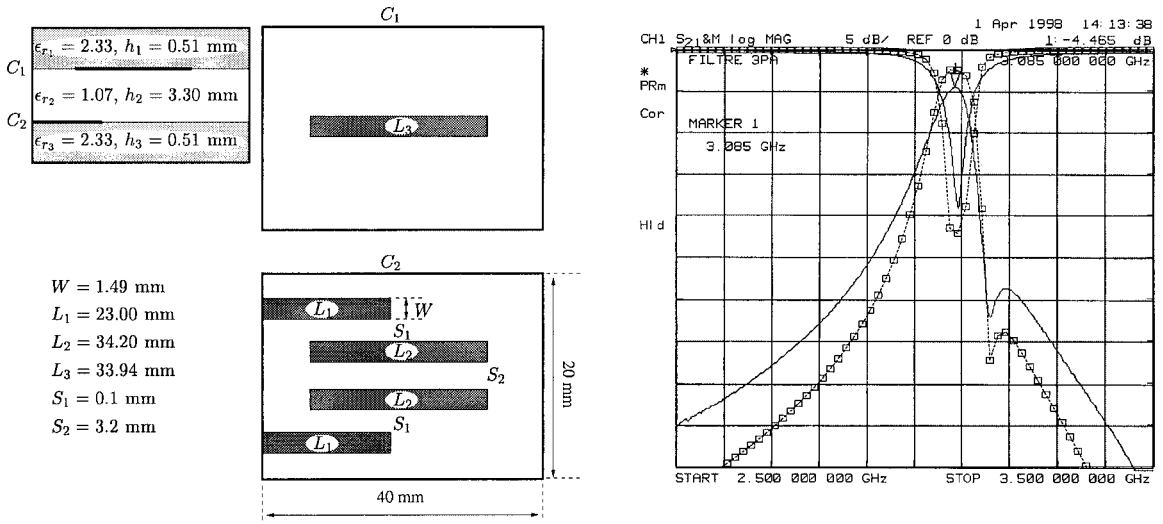

(a) Geometry of the filter.

(b) Measured versus simulated results.

Figure 5 Filter with transmission zero above the passband due to a cross coupling between first and third resonators. Square points are simulations, while solid lines are measurements

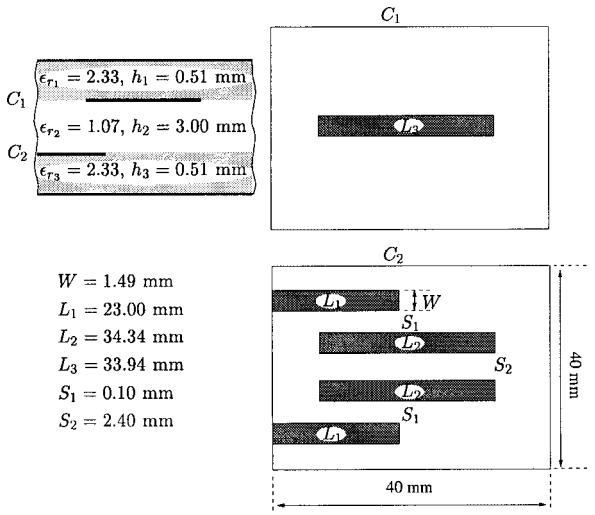

(a) Geometry of the filter.

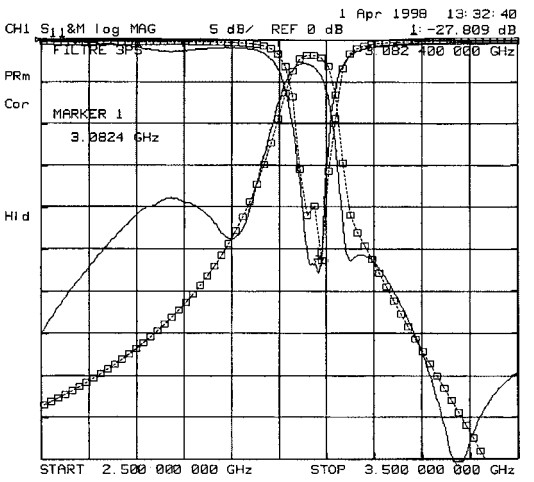

(b) Measured versus simulated results.

Figure 6 Filter with transmission zero using the 1–3 cross-coupling concept, but with no lateral cavity walls. Square points are simulations, while solid lines are measurements

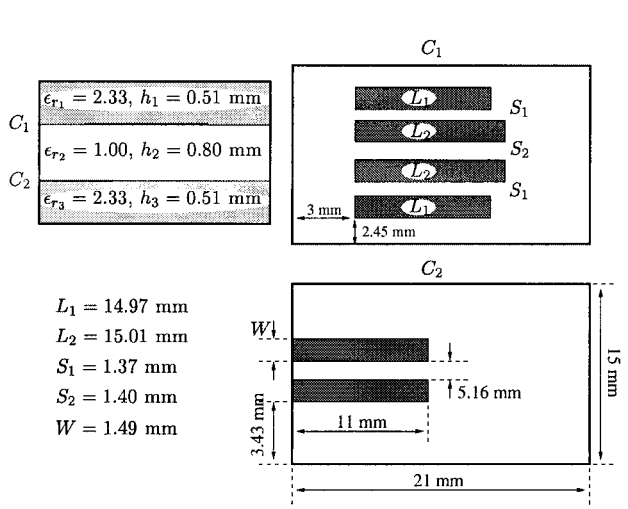

(a) Geometry of the filter.

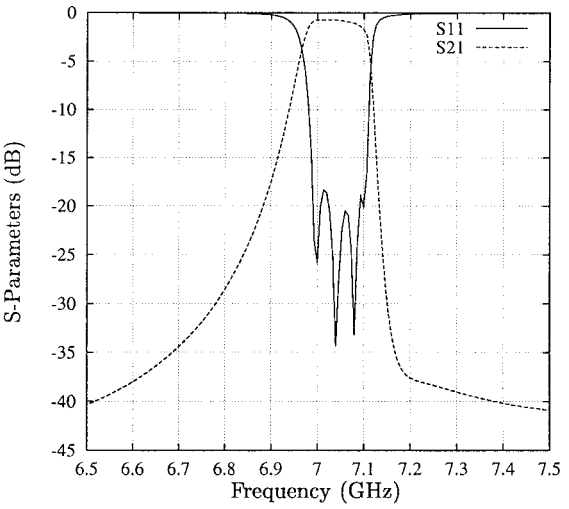

(b) Electrical response.

Figure 7 Bandpass filter optimized for high selectivity above the passband, using dispersive behavior mode interactions

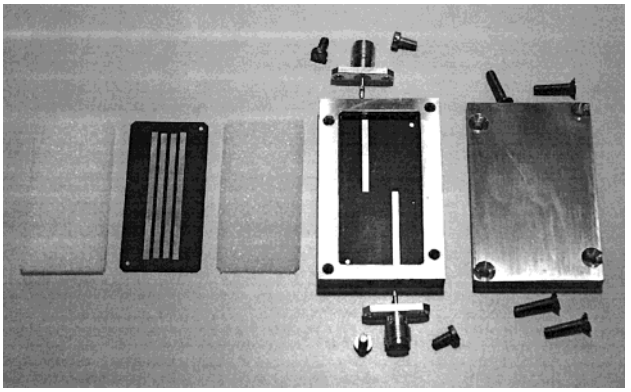

Figure 8 Aspect of the manufactured breadboard, showing all pieces of the filter

due to the difficulty in changing the sign of the needed cross coupling. To overcome this limitation, alternative structures for the implementation of transmission zeros were investigated. Figure 7 presents a multilayered structure with all resonators printed on the same dielectric, but the input and output lines are placed on a different substrate, which is separated from the resonator level by a layer of air. Figure 7(b) presents the electrical behavior of the structure, showing a transmission zero above the passband of the filter.

The presence of this transmission zero can be attributed to the dispersive nature of the modes excited in the structure, whose interactions produce a cancellation of energy above the passband. The interesting feature of this structure is that the sign of the coupling can now be easily changed by simply placing an additional layer of air on top. This additional layer actually increases the propagation velocity of the modes, which causes the cancellation of energy to take place this time below the passband.

In Figure 8, we present a filter prototype manufactured in our laboratory following this last idea. In the figure, all of the pieces of the filter can be observed, including the foam substrates with $\epsilon_r = 1.07$ used to model the air layers. Figure 9 presents the final optimized dimensions, together with the electrical response of the filter, showing the transmission zero and corresponding selectivity improvement below the passband. The figure also presents measured versus simulated results, showing that the agreement is also very good in this case.

In connection with this last structure, it is interesting to note that the dispersive nature of the excited modes can be easily modified by introducing a slot on the top lid of the cavity. In this way, the cancellation of energy can be adjusted to produce a transmission zero above or below the passband of the filter, as desired. To show the capability of a slot to tune the position of the transmission zero, we present in Figure 10 a microwave filter of order 2 with an additional slot open on the top lid of the box. Figure 10 also shows the responses of the filter for three different positions of the slot. In Figure 10(b), the slot is close to the lateral walls, and its effects are therefore negligible. The structure presents a transmission zero below the passband, as in the previous case. As the position of the slot is varied, the transmission zero shifts with respect to the passband of the filter, and in Figure 10(c), it lies in the middle of the frequency band. If the slot continues to vary, the transmission zero shifts again, until eventually it moves above the passband, as clearly shown in Figure 10(d).

4. CONCLUSIONS

In this paper, a number of novel microstrip filter structures have been investigated. In particular, the advantages and effects of introducing broadside couplings between resonators have been studied. It has been found that the level of coupling achieved when the resonators are placed broadside is considerably higher as compared with the side-coupled counterparts.

In addition, broadside-coupled structures allow us to easily introduce cross couplings between nonadjacent resonators, thus resulting in the implementation of transmission zeros in the insertion loss response of microwave filters. In this paper, several interesting structures for the implementation of transmission zeros have been introduced and discussed. In particu-

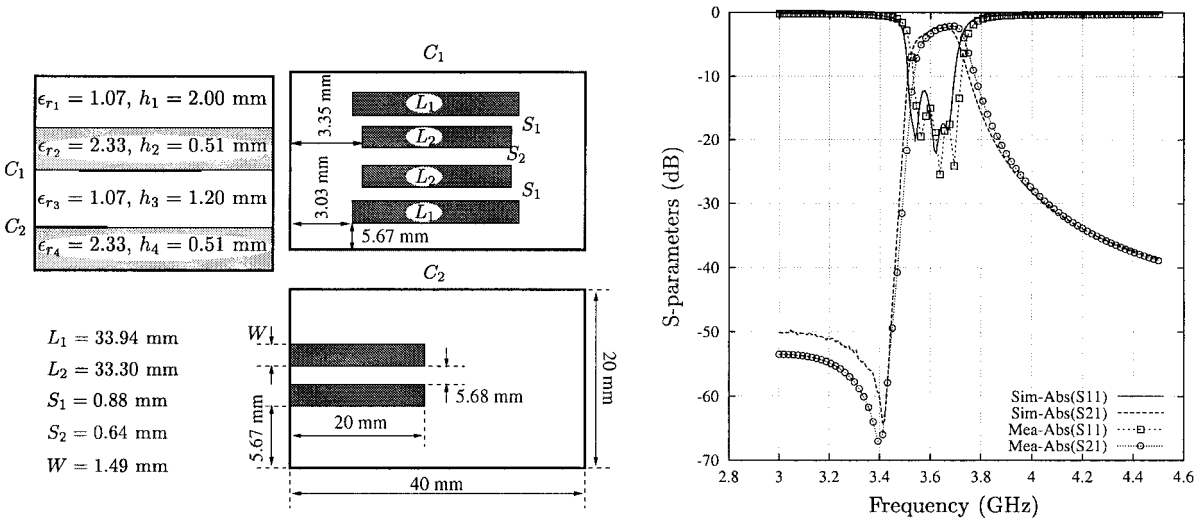

(a) Geometry of the filter.

(b) Electrical response.

Figure 9 Bandpass filter optimized for high selectivity below the passband, using dispersive behavior mode interactions. Measured results are also shown

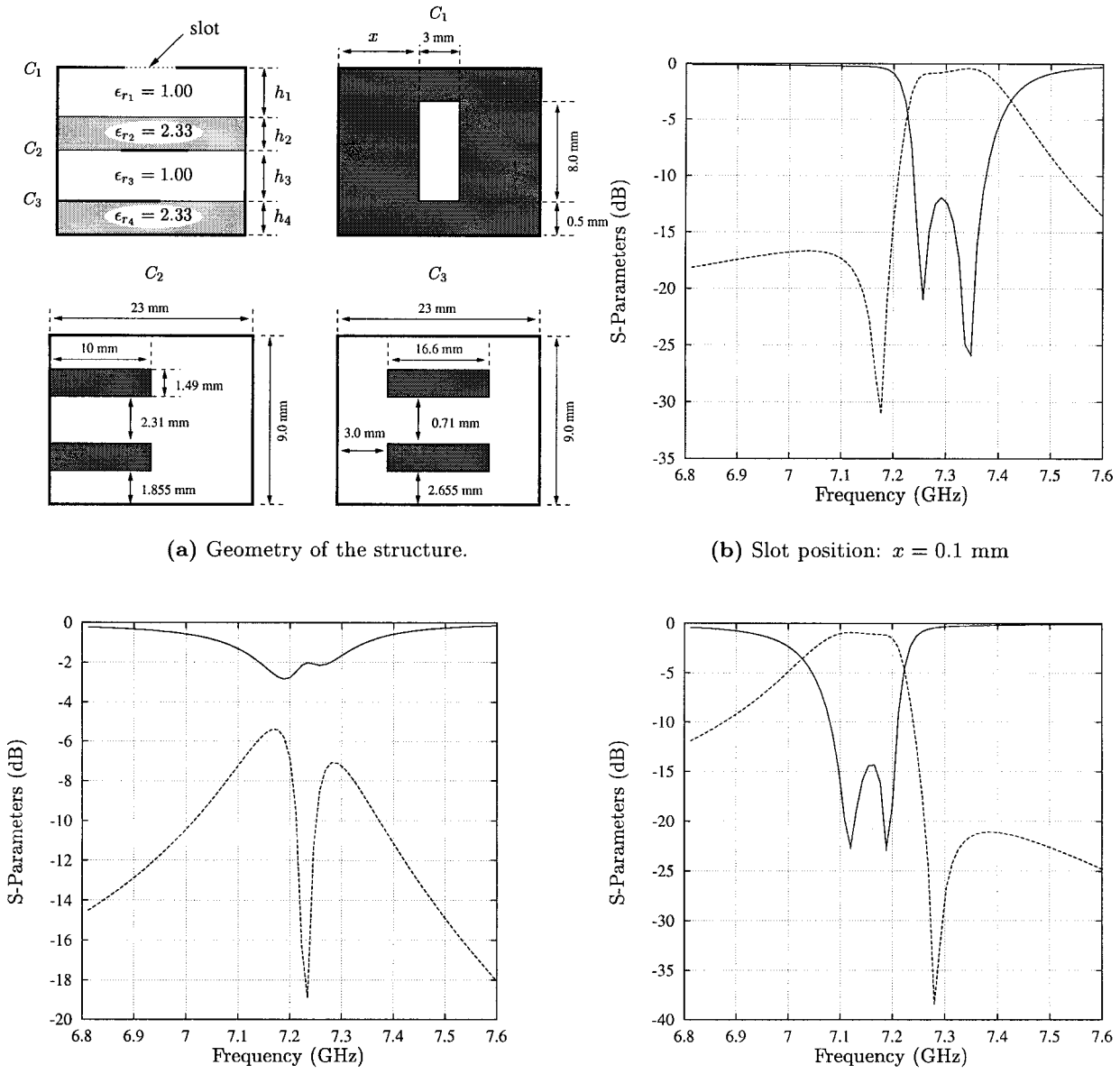

(a) Geometry of the structure.

(b) Slot position: $x = 0.1$ mm

(c) Slot position: $x = 5.0$ mm

(d) Slot position: $x = 7.0$ mm

Figure 10 Second-order filter with transmission zero and slot open on top of the box ($h_1 = 2.0$ mm, $h_2 = 0.51$ mm, $h_3 = 1.7$ mm, $h_4 = 0.51$ mm)

lar, the implementation of transmission zeros both above and below the filter bandpass have been demonstrated.

Finally, several filter structures have been manufactured and tested, and comparisons with theory have been presented. Good agreement with predicted results has been obtained, thus confirming the validity of the new structures proposed.

REFERENCES

1. E.R. Soares, J.D. Fuller, P.J. Marozick, and R.L. Alvarez, Applications of high-temperature-superconducting filters and cryoelectronics for satellite communication, IEEE Trans Microwave Theory Tech 48 (2000), 1190–1198.
2. G.L. Matthaei, J.C. Rautio, and B.A. Willemsen, Concerning the influence of housing dimensions on the response and design of microstrip filters with parallel-line couplings, IEEE Trans Microwave Theory Tech 48 (2000), 1361–1368.
3. M.D. Vincentis, J. Kim, Y. Qian, G. Feng, P. Ma, M.F. Chang, and T. Itoh, A multilayer integration technique for low-loss, low-crosstalk interconnections and circuits for rf silicon mmics, Proc 30th European Microwave Conf EuMC'2000, Paris, France, Oct. 2000, vol. 2, pp. 25–28.
4. E.G. Krantz and G.R. Branner, Active microwave filters with noise performance considerations, IEEE Trans Microwave Theory Tech 42 (1994), 1368–1379.
5. B.J. Minnis, Classes of sub-miniature microwave printed filters with arbitrary passband and stopband width, IEEE Trans Microwave Theory Tech MTT-30 (1982), 1893–1900.
6. G. Subramanyam, F.W.V. Keuls, and F.A. Miranda, A K-band-

frequency agile microstrip bandpass filter using a thin-film HTS/ferroelectric/dielectric multilayer configuration, IEEE Trans Microwave Theory Tech 48 (2000), 525–530.
7. J.-S. Hong, M.J. Lancaster, D. Jedamzik, R.B. Greed, and J.-C. Mage, On the performance of HTS microstrip quasi-elliptic function filters for mobile communication application, IEEE Trans Microwave Theory Tech 48 (2000), 1240–1246.
8. G.L. Matthaei, N.O. Fenzi, R.J. Forse, and S.M. Rohlfing, Hairpin-comb filters for HTS and other narrow-band applications, IEEE Trans Microwave Theory Tech 45 (1997), 1226–1231.
9. R.M. Kurzok, General four-resonator filters at microwave frequencies, IEEE Trans Microwave Theory Tech MTT-14 (1966), 295–296.
10. A.E. Atia and A.E. Williams, Narrow-bandpass waveguide filters, IEEE Trans Microwave Theory Tech MTT-20 (1972), 258–265.
11. R. Levy, Filters with single transmission zeros at real and imaginary frequencies, IEEE Trans Microwave Theory Tech MTT-24 (1976), 172–181.
12. J.-F. Liang, X.P. Liang, K.A. Zaki, and A.E. Atia, Dual-mode dielectric or air-filled rectangular waveguide filters, IEEE Trans Microwave Theory Tech 43 (1995), 2824–2830.
13. M. Guglielmi, F. Montauti, L. Pellegrini, and P. Arcioni, Implementing transmission zeros in inductive-window bandpass filters, IEEE Trans Microwave Theory Tech 43 (1995), 1911–1915.
14. C. Wang, K.A. Zaki, and A.E. Atia, Dual-mode conductor-loaded cavity filters, IEEE Trans Microwave Theory Tech 45 (1997), 1240–1246.
15. J.-S. Hong and M.J. Lancaster, Design of highly selective microstrip bandpass filters with a single pair of attenuation poles at finite frequencies, IEEE Trans Microwave Theory Tech 48 (2000), 1098–1107.
16. J.-S. Hong and M.J. Lancaster, Couplings of microstrip square open-loop resonators for cross-coupled planar microwave filters, IEEE Trans Microwave Theory Tech 44 (1996), 2099–2109.
17. C.C. Yu and K. Chang, Novel compact elliptic-function narrow-band bandpass filters using microstrip open-loop resonators with coupled and crossing lines, IEEE Trans Microwave Theory Tech 46 (1998), 952–958.
18. J.-S. Hong and M.J. Lancaster, Cross-coupled microstrip hairpin-resonator filters, IEEE Trans Microwave Theory Tech 46 (1998), 118–122.
19. M. Tsuji and H. Shigesawa, Spurious response suppression in broadband and introduction of attenuation poles as guard bands in printed-circuit filters, Proc 30th European Microwave Conference, EuMC' 2000, Paris, France, Oct. 2000, pp. 44–47.
20. H. Okazaki and T. Hirota, Multilayer MMIC broad-side coupler with a symmetric structure, IEEE Microwave Guided Wave Lett 7 (1997), 145–146.
21. S.-J. Yao, R.R. Bonetti, and A.E. Williams, Generalized dual-plane multicoupled line filters, IEEE Trans Microwave Theory Tech 41 (1993), 2182–2189.
22. J.-S. Hong and M.J. Lancaster, Aperture-coupled microstrip open-loop resonators and their applications to the design of novel microstrip bandpass filters, IEEE Trans Microwave Theory Tech 47 (1999), 1848–1855.
23. J.A. Curtis and S.J. Fiedziusko, Multi-layered planar filters based on aperture coupled, dual mode microstrip of stripline resonators, IEEE MTT-S Dig, June 1992, pp. 1203–1206.
24. S.J. Yao and R.R. Bonetti, Dual-plane coupled-line microwave filter, IEEE MTT-S Dig, June 1993.
25. A. Alvarez-Melcón, J.R. Mosig, and M. Guglielmi, Efficient CAD of boxed microwave circuits based on arbitrary rectangular elements, IEEE Trans Microwave Theory Tech (Dec. 1998, accepted).
26. S.B. Cohn, Parallel-coupled transmission-line-resonator filters, IEEE Trans Microwave Theory Tech MTT-6 (1958).
27. G.I. Zysman and A.K. Johnson, Coupled transmission line networks and coupling structures, IEEE Trans Microwave Theory Tech MTT-17 (1969).
28. C.-Y. Chang and T. Itoh, A modified parallel-coupled filter structure that improves the upper stopband rejection and response symmetry, IEEE Trans Microwave Theory Tech 39 (1991), 310–314.
29. I. Shapir, V.A. Sharir, and D.G. Swanson, TEM modeling of parasitic bandwidth expansion in combline filter, IEEE Trans Microwave Theory Tech 47 (1999), 1664–1669.
30. R. Levy, H.-W. Yao, and K.A. Zaki, Transitional combline/evanescent-mode microwave filters, IEEE Trans Microwave Theory Tech 45 (1997), 2094–2099.
31. G.L. Matthaei, Combline band-pass filters of narrow or moderate bandwidth, Microwave J 6 (1963), 82–91.
32. D. Chambers and J.D. Rhodes, Asymmetric synthesis of microwave filters, Proc 11th European Microwave Conf, EuMC, Amsterdam, The Netherlands, Sept. 1981, pp. 105–110.

DISTRIBUTED INDUCTANCE AND RESISTANCE PER-UNIT-LENGTH FORMULAS FOR VLSI INTERCONNECTS ON SILICON SUBSTRATE

H. Ymeri,[1] B. Nauwelaers,[1] and Karen Maex[1, 2]
[1]Department of Electrical Engineering (ESAT)
Div. ESAT-TELEMIC
Katholieke Universiteit Leuven
B-3001 Leuven-Heverlee, Belgium
[2]IMEC
B-3001 Leuven, Belgium

Received 23 March 2001

ABSTRACT: *A new analytic model is presented (the model is based on the induced current density distribution inside silicon substrate) to calculate the frequency-dependent distributed inductance and the associated distributed series resistance of silicon semiconducting VLSI interconnects. The validity of the proposed model has been checked by a comparison with CAD-oriented modeling methodology in conjunction with a quasi-TEM spectral-domain approach. It is found that the silicon semiconducting substrate skin effect must be considered for the accurate prediction of the high-frequency characteristics of VLSI interconnects.*
© 2001 John Wiley & Sons, Inc. Microwave Opt Technol Lett 30: 302–304, 2001.

Key words: *VLSI interconnect; magnetic potential; distributed inductance and resistance; lossy silicon substrate*

1. INTRODUCTION

As the density, complexity, and speed of VLSI circuits are continuing to increase, the management of the on-chip interconnects becomes of paramount concern to the IC designer, especially with respect to the internal parasitics parameters' immunity [1]. In order to accomplish this, it is necessary to analyze and model the broadband characteristics [2–6, 9] of the silicon VLSI interconnects since the signals tend to exhibit both short rising and falling times. For the case of silicon, the effect of the high-loss substrate on the distributed inductance and resistance of the interconnects has not been modeled well with analytical closed-form expressions. In this letter, we suggest an analytical model (based on silicon-substrate-induced current distribution) that can accurately predict the frequency-dependent inductance and resistance of silicon-substrate IC interconnects, with good agreement with the quasi-TEM spectral-domain approach and full-wave numerical simulation over a wide range of dimensions, substrate conductivity, and frequency.